Anomalous Hall Effect for Electrons in ^{3}He-A

A Sensitive Probe of the Quasiparticle-Ion T-matrix

Oleksii Shevtsov James A. Sauls

Northwestern University, Evanston, IL 60208 USA

March 16, 2017

(1) Intro: transport of *e*-bubbles in superfluid ^{3}He

(2) Potential models for *e*-bubbles

(3) Comparison of models [Shevtsov and Sauls, JLTP (2016)]

DMR-1508730

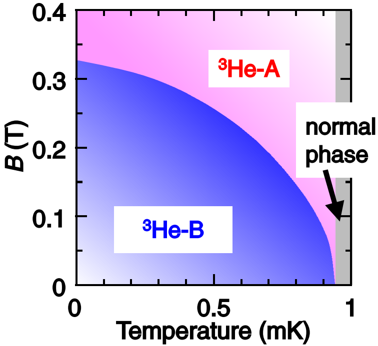

Ikegami et al. J. Phys. Soc. Jpn. **84**, 044602 (2015)

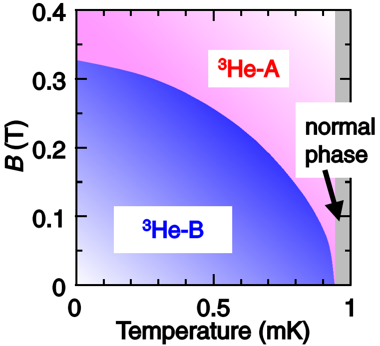

Ikegami et al. J. Phys. Soc. Jpn. **84**, 044602 (2015)

ABM state (A-phase): $L_z = 1, S_z = 0$

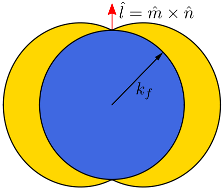

$$\hat{\mathbf{l}} \parallel \hat{\mathbf{z}}: \ \Delta(\hat{\mathbf{k}}) = \Delta \sigma_x (\hat{k}_x + i\hat{k}_y)/k_f$$

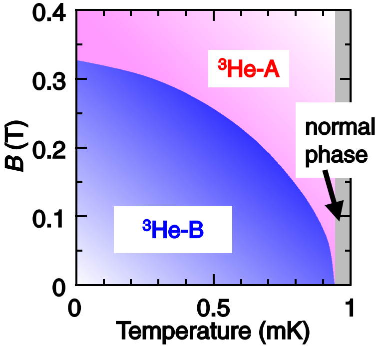

Ikegami et al. J. Phys. Soc. Jpn. **84**, 044602 (2015)

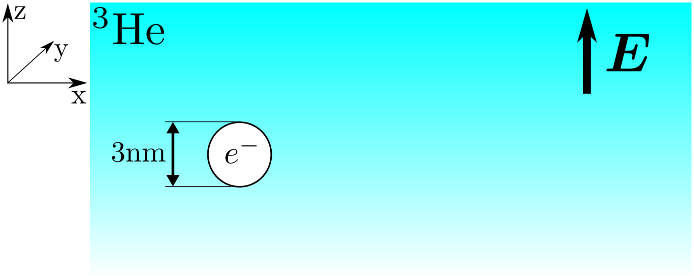

- Bubble with $R \simeq 1.5$ nm, $\lambda_f \ll R \ll \xi_0$
- Effective mass $M \simeq 100 m_3$ (m_3 – atomic mass of ^{3}He)

ABM state (A-phase): $L_z = 1, S_z = 0$

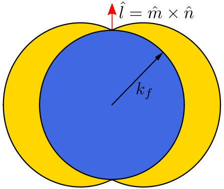

$$\hat{\mathbf{l}} \parallel \hat{\mathbf{z}}: \ \Delta(\hat{\mathbf{k}}) = \Delta \sigma_x (\hat{k}_x + i\hat{k}_y)/k_f$$

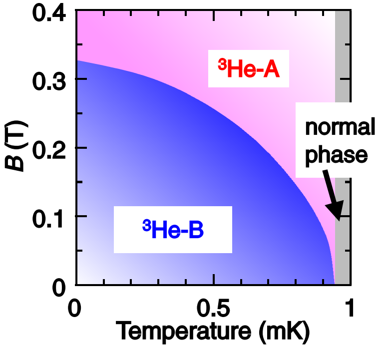

Ikegami et al. J. Phys. Soc. Jpn. **84**, 044602 (2015)

ABM state (A-phase): $L_z = 1, S_z = 0$

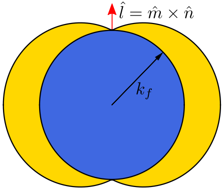

$\hat{\mathbf{l}} \parallel \hat{\mathbf{z}}: \ \Delta(\hat{\mathbf{k}}) = \Delta\sigma_x(\hat{k}_x + i\hat{k}_y)/k_f$

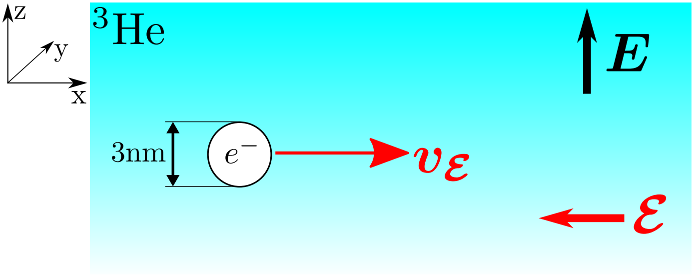

- Bubble with $R \simeq 1.5$ nm, $\lambda_f \ll R \ll \xi_0$
- Effective mass $M \simeq 100 m_3$ (m_3 – atomic mass of ^{3}He)
- QPs mean free path $l \gg R$, Knudsen limit
- Normal-state mobility is const below $T = 50$ mK

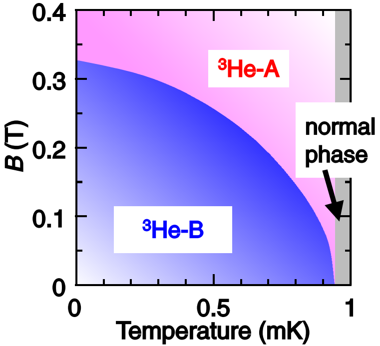

Ikegami et al. J. Phys. Soc. Jpn. **84**, 044602 (2015)

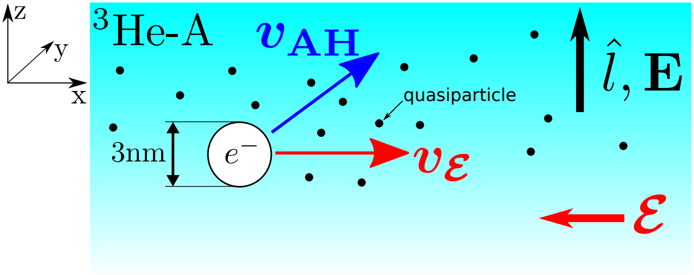

Electric current: $\mathbf{v} = \overbrace{\mu_\perp \boldsymbol{\mathcal{E}}}^{\mathbf{v}_{\mathcal{E}}} + \overbrace{\mu_{\mathrm{AH}} \boldsymbol{\mathcal{E}} \times \hat{\mathbf{l}}}^{\mathbf{v}_{\mathrm{AH}}}$ Salmelin, Salomaa & Mineev (1989)

Hall ratio: $\tan\alpha = v_{\mathrm{AH}}/v_{\mathcal{E}} = |\mu_{\mathrm{AH}}/\mu_\perp|$

ABM state (A-phase): $L_z = 1, S_z = 0$

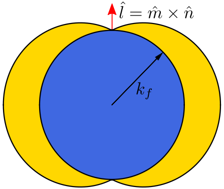

$\hat{\mathbf{l}} \parallel \hat{\mathbf{z}}: \ \Delta(\hat{\mathbf{k}}) = \Delta \sigma_x (\hat{k}_x + i\hat{k}_y)/k_f$

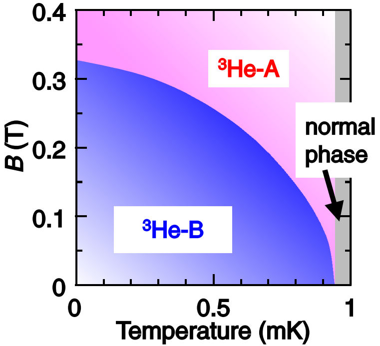

Ikegami et al. J. Phys. Soc. Jpn. **84**, 044602 (2015)

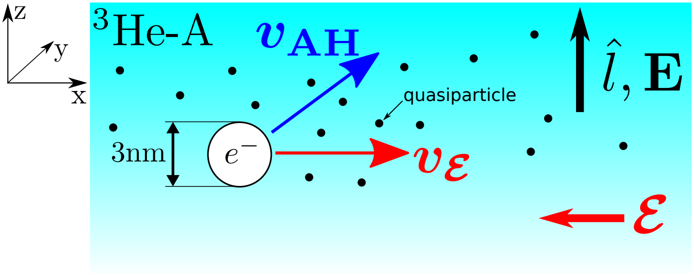

ABM state (A-phase): $L_z = 1, S_z = 0$

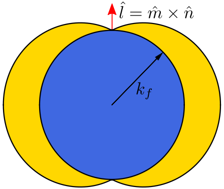

$\hat{\mathbf{l}} \parallel \hat{\mathbf{z}}$: $\Delta(\hat{\mathbf{k}}) = \Delta\sigma_x(\hat{k}_x + i\hat{k}_y)/k_f$

Electric current: $\mathbf{v} = \overbrace{\mu_\perp \boldsymbol{\mathcal{E}}}^{\mathbf{v}_{\mathcal{E}}} + \overbrace{\mu_{\mathrm{AH}} \boldsymbol{\mathcal{E}} \times \hat{\mathbf{l}}}^{\mathbf{v}_{\mathrm{AH}}}$ Salmelin, Salomaa & Mineev (1989)

Hall ratio: $\tan\alpha = v_{\mathrm{AH}}/v_{\mathcal{E}} = |\mu_{\mathrm{AH}}/\mu_\perp|$

Equation of motion: $M\dot{\mathbf{v}} = e\boldsymbol{\mathcal{E}} - \overleftrightarrow{\eta} \cdot \mathbf{v}$, $\overleftrightarrow{\eta}$ – Stokes tensor

Stationary state: $\mathbf{v} = \overleftrightarrow{\mu} \cdot \boldsymbol{\mathcal{E}} \rightsquigarrow \overleftrightarrow{\mu} = e\overleftrightarrow{\eta}^{-1}$

$$\overleftrightarrow{\eta} = \begin{pmatrix} \eta_\perp & \eta_{\mathrm{AH}} & 0 \\ -\eta_{\mathrm{AH}} & \eta_\perp & 0 \\ 0 & 0 & \eta_\parallel \end{pmatrix},$$

$\eta_\perp$ – longitudinal component

η_{AH} – anomalous Hall component

(i) Lippmann-Schwinger equation for the retarded T-matrix:

$$\hat{T}_S^R(\mathbf{k}',\mathbf{k},E) = \hat{T}_N^R(\mathbf{k}',\mathbf{k}) + \int \frac{d^3k''}{(2\pi)^3}\, \hat{T}_N^R(\mathbf{k}',\mathbf{k}'')\Big[\hat{G}_S^R(\mathbf{k}'',E) - \hat{G}_N^R(\mathbf{k}'',E)\Big]\hat{T}_S^R(\mathbf{k}'',\mathbf{k},E)$$

(i) Lippmann-Schwinger equation for the retarded T-matrix:

$$\hat{T}_S^R(\mathbf{k}', \mathbf{k}, E) = \hat{T}_N^R(\mathbf{k}', \mathbf{k}) + \int \frac{d^3k''}{(2\pi)^3} \hat{T}_N^R(\mathbf{k}', \mathbf{k}'') \Big[\hat{G}_S^R(\mathbf{k}'', E) - \hat{G}_N^R(\mathbf{k}'', E) \Big] \hat{T}_S^R(\mathbf{k}'', \mathbf{k}, E)$$

(ii) QP-ion potential: $V(r) \rightsquigarrow$ phase shifts $\{\delta_l, l = 0, 1, \dots\} \rightsquigarrow \hat{T}_N^R(\mathbf{k}', \mathbf{k})$

(i) Lippmann-Schwinger equation for the retarded T-matrix:

$$\hat{T}_S^R(\mathbf{k}',\mathbf{k},E)=\hat{T}_N^R(\mathbf{k}',\mathbf{k})+\int\frac{d^3k''}{(2\pi)^3}\,\hat{T}_N^R(\mathbf{k}',\mathbf{k}'')\Big[\hat{G}_S^R(\mathbf{k}'',E)-\hat{G}_N^R(\mathbf{k}'',E)\Big]\hat{T}_S^R(\mathbf{k}'',\mathbf{k},E)$$

(ii) QP-ion potential: $V(r) \rightsquigarrow$ phase shifts $\{\delta_l, l=0,1,\dots\} \rightsquigarrow \hat{T}_N^R(\mathbf{k}',\mathbf{k})$

(iii) Golden rule: $\Gamma(\mathbf{k}',\mathbf{k})=\frac{2\pi}{\hbar}\sum_{\mathrm{in,out}}|\langle \mathrm{out}_{\mathbf{k}'}|\hat{T}_S|\mathrm{in}_{\mathbf{k}}\rangle|^2\delta(E_{\mathbf{k}'}-E_{\mathbf{k}}) \rightsquigarrow$ drag force $\mathbf{F}_{QP}=-\overleftrightarrow{\eta}\cdot\mathbf{v}$

(i) Lippmann-Schwinger equation for the retarded T-matrix:

$$\hat{T}_S^R(\mathbf{k}',\mathbf{k},E) = \hat{T}_N^R(\mathbf{k}',\mathbf{k}) + \int \frac{d^3k''}{(2\pi)^3}\,\hat{T}_N^R(\mathbf{k}',\mathbf{k}'')\Big[\hat{G}_S^R(\mathbf{k}'',E) - \hat{G}_N^R(\mathbf{k}'',E)\Big]\hat{T}_S^R(\mathbf{k}'',\mathbf{k},E)$$

(ii) QP-ion potential: $V(r) \rightsquigarrow$ phase shifts $\{\delta_l, l = 0, 1, \ldots\} \rightsquigarrow \hat{T}_N^R(\mathbf{k}',\mathbf{k})$

(iii) Golden rule: $\Gamma(\mathbf{k}',\mathbf{k}) = \dfrac{2\pi}{\hbar}\sum_{\mathrm{in,out}} |\langle \mathrm{out}_{\mathbf{k}'}|\,\hat{T}_S|\mathrm{in}_{\mathbf{k}}\rangle|^2 \delta(E_{\mathbf{k}'} - E_{\mathbf{k}}) \rightsquigarrow$ drag force $\mathbf{F}_{QP} = -\overleftrightarrow{\eta}\cdot\mathbf{v}$

(iv) Hard sphere: $\tan\delta_l = j_l(k_f R)/n_l(k_f R)$

(i) Lippmann-Schwinger equation for the retarded T-matrix:

$$\hat{T}_S^R(\mathbf{k}',\mathbf{k},E)=\hat{T}_N^R(\mathbf{k}',\mathbf{k})+\int\frac{d^3k''}{(2\pi)^3}\hat{T}_N^R(\mathbf{k}',\mathbf{k}'')\Big[\hat{G}_S^R(\mathbf{k}'',E)-\hat{G}_N^R(\mathbf{k}'',E)\Big]\hat{T}_S^R(\mathbf{k}'',\mathbf{k},E)$$

(ii) QP-ion potential: $V(r)\rightsquigarrow$ phase shifts $\{\delta_l, l=0,1,\dots\}\rightsquigarrow \hat{T}_N^R(\mathbf{k}',\mathbf{k})$

(iii) Golden rule: $\Gamma(\mathbf{k}',\mathbf{k})=\frac{2\pi}{\hbar}\sum_{\mathrm{in,out}}|\langle \mathrm{out}_{\mathbf{k}'}|\hat{T}_S|\mathrm{in}_{\mathbf{k}}\rangle|^2\delta(E_{\mathbf{k}'}-E_{\mathbf{k}})\rightsquigarrow$ drag force $\mathbf{F}_{QP}=-\overleftrightarrow{\eta}\cdot\mathbf{v}$

(iv) Hard sphere: $\tan\delta_l=j_l(k_fR)/n_l(k_fR)$ [also recall: $\overleftrightarrow{\mu}=e\overleftrightarrow{\eta}^{-1}$, $\tan\alpha=\mu_{\mathrm{AH}}/\mu_\perp$]

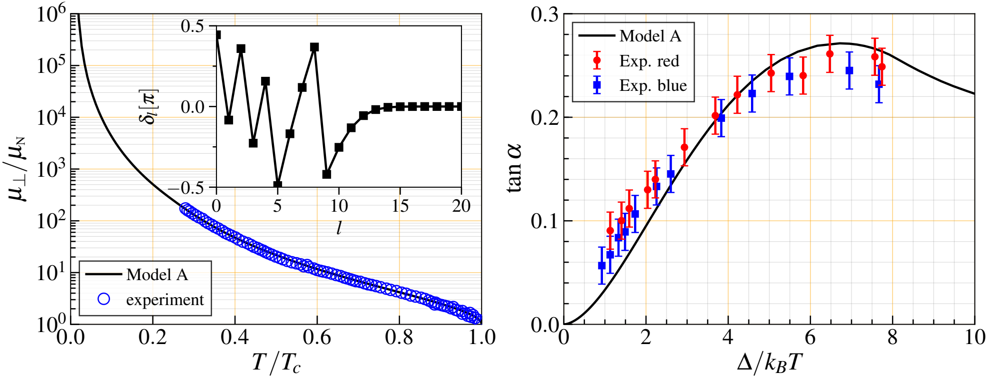

Experiments:

Ikegami et al. (RIKEN)

Science **341**, 59 (2013)

JPSJ **82**, 124607 (2013)

JPSJ **84**, 044602 (2015)

Theory:

Shevtsov & Sauls

PRB **94**, 064511 (2016)

Alternative QP-ion scattering potential models

Alternative QP-ion scattering potential models

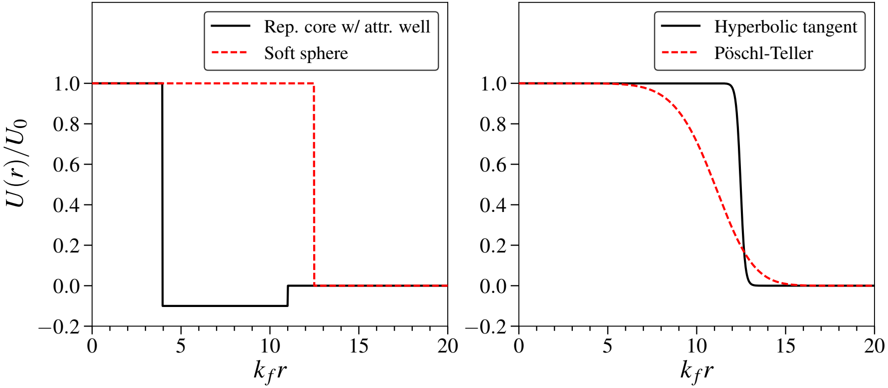

Repulsive core w/ attr. well:

$$U(r) = \begin{cases} U_0, & r < R, \\ -U_1, & R < r < R', \\ 0, & r > R'. \end{cases}$$

Pöschl-Teller potential:

$U(x) = U_0/\cosh^2[\alpha x^n]$

Hyperbolic tangent:

$U(x) = U_0[1 - \tanh(\frac{x-b}{c})]/2$,
$x = k_f r$

Alternative QP-ion scattering potential models

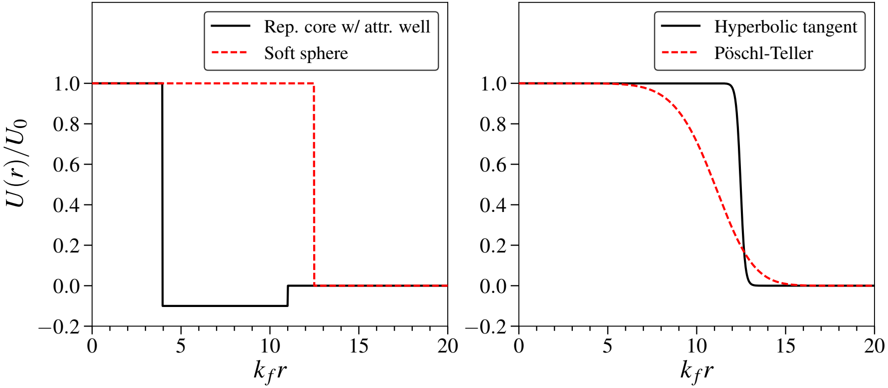

Repulsive core w/ attr. well:

$$U(r) = \begin{cases} U_0, & r < R, \\ -U_1, & R < r < R', \\ 0, & r > R'. \end{cases}$$

Pöschl-Teller potential:
$U(x) = U_0/\cosh^2[\alpha x^n]$

Hyperbolic tangent:
$U(x) = U_0[1 - \tanh(\frac{x-b}{c})]/2,$
$x = k_f r$

(i) Compute phase shifts: analytically or via variable-phase approach (F. Calogero 1967)

Alternative QP-ion scattering potential models

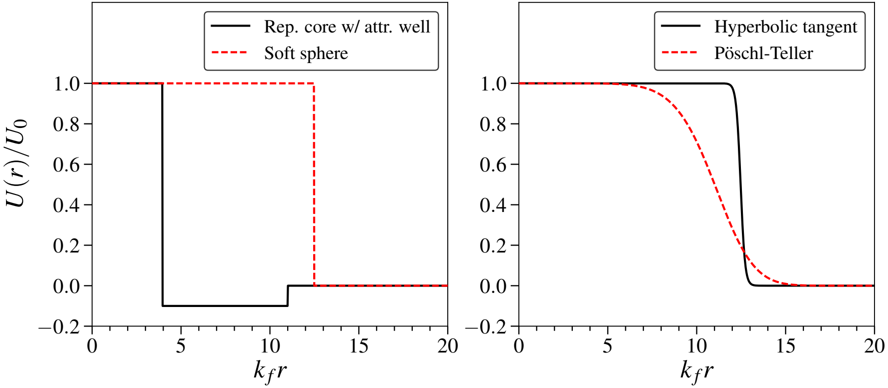

Repulsive core w/ attr. well:

$$U(r) = \begin{cases} U_0, & r < R, \\ -U_1, & R < r < R', \\ 0, & r > R'. \end{cases}$$

Pöschl-Teller potential:

$U(x) = U_0 / \cosh^2[\alpha x^n]$

Hyperbolic tangent:

$U(x) = U_0[1 - \tanh(\frac{x-b}{c})]/2$,

$x = k_f r$

(i) Compute phase shifts: analytically or via variable-phase approach (F. Calogero 1967)

(ii) Transport cross section: $\sigma_N = (4\pi/k_f^2) \sum_{l=0}^{\infty} (l+1) \sin^2(\delta_{l+1} - \delta_l)$

Alternative QP-ion scattering potential models

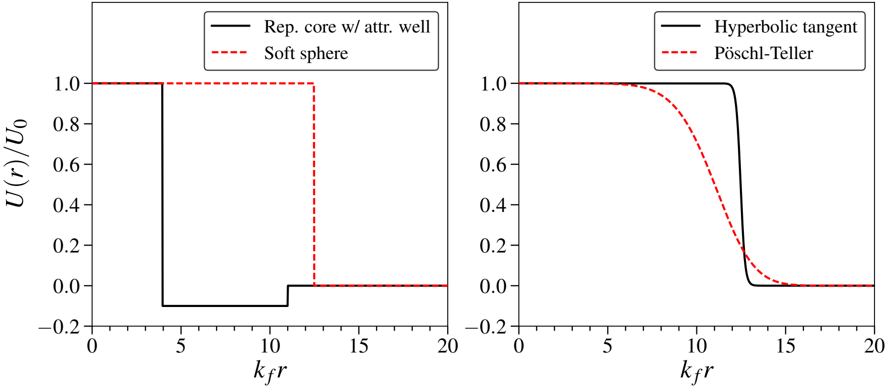

Repulsive core w/ attr. well:

$$U(r) = \begin{cases} U_0, & r < R, \\ -U_1, & R < r < R', \\ 0, & r > R'. \end{cases}$$

Pöschl-Teller potential:
$U(x) = U_0 / \cosh^2[\alpha x^n]$

Hyperbolic tangent:
$U(x) = U_0[1 - \tanh(\frac{x-b}{c})]/2$,
$x = k_f r$

(i) Compute phase shifts: analytically or via variable-phase approach (F. Calogero 1967)

(ii) Transport cross section: $\sigma_N = (4\pi/k_f^2) \sum_{l=0}^{\infty} (l+1) \sin^2(\delta_{l+1} - \delta_l)$

(iii) Fit the normal-state mobility: $\mu_N = e/(n_3 p_f \sigma_N) \rightsquigarrow \mu_N^{\rm exp} = 1.7 \times 10^{-6}\, m^2/V\,s$

Alternative QP-ion scattering potential models

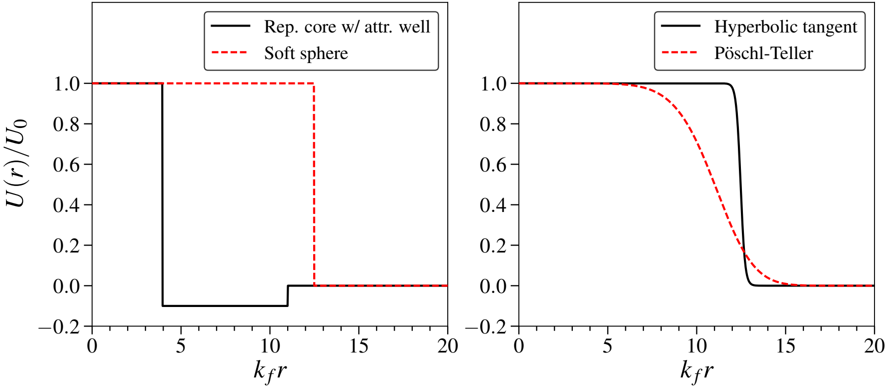

Repulsive core w/ attr. well:

$$U(r) = \begin{cases} U_0, & r < R, \\ -U_1, & R < r < R', \\ 0, & r > R'. \end{cases}$$

Pöschl-Teller potential:

$U(x) = U_0 / \cosh^2[\alpha x^n]$

Hyperbolic tangent:

$U(x) = U_0[1 - \tanh(\frac{x-b}{c})]/2$, $x = k_f r$

(i) Compute phase shifts: analytically or via variable-phase approach (F. Calogero 1967)

(ii) Transport cross section: $\sigma_N = (4\pi/k_f^2) \sum_{l=0}^{\infty} (l+1) \sin^2(\delta_{l+1} - \delta_l)$

(iii) Fit the normal-state mobility: $\mu_N = e/(n_3 p_f \sigma_N) \rightsquigarrow \mu_N^{\text{exp}} = 1.7 \times 10^{-6}\, m^2/V\, s$

Hard sphere model (model A) is chosen as a benchmark for other potential models!

Model B: repulsive core with attractive well

- $U(r) = \begin{cases} U_0, & r < R, \\ -U_1, & R < r < R', \\ 0, & r > R'. \end{cases} \quad U_0 = 100E_f, U_1 = 10E_f, k_f R' = 11, R/R' = 0.36$

- $\overleftrightarrow{\mu} = \begin{pmatrix} \mu_\perp & \mu_{\mathrm{AH}} & 0 \\ -\mu_{\mathrm{AH}} & \mu_\perp & 0 \\ 0 & 0 & \mu_\parallel \end{pmatrix}, \quad \tan\alpha = \frac{\mu_{\mathrm{AH}}}{\mu_\perp}$

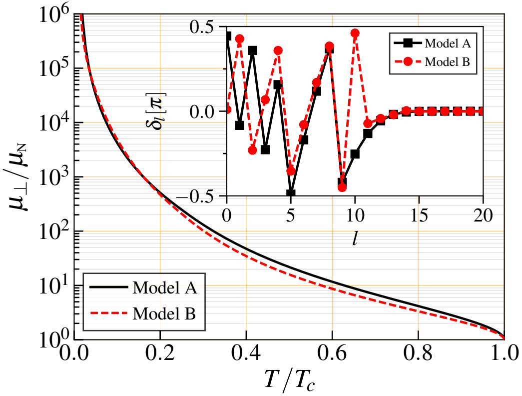

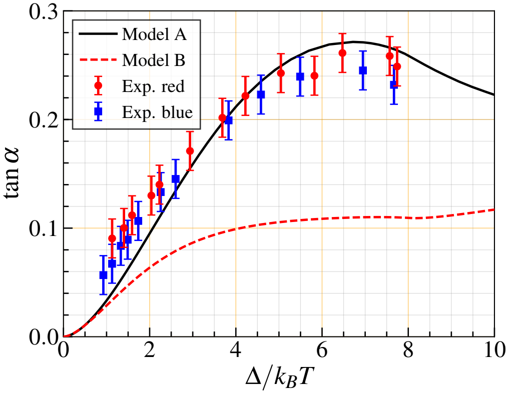

Models C and D: random phase shifts

- We fix $l_{\max} = 11$ and use random number generator for $\{\delta_l | l = 1, 2, \ldots, l_{\max}\}$; the remaining δ_0 is adjusted to fit $\mu_N^{\exp}$(Models C and D differ by seed)
- $$\overleftrightarrow{\mu} = \begin{pmatrix} \mu_\perp & \mu_{\mathrm{AH}} & 0 \\ -\mu_{\mathrm{AH}} & \mu_\perp & 0 \\ 0 & 0 & \mu_\| \end{pmatrix}, \quad \tan\alpha = \frac{\mu_{\mathrm{AH}}}{\mu_\perp}$$

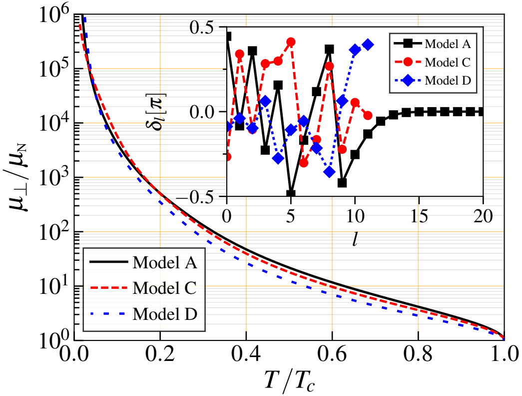

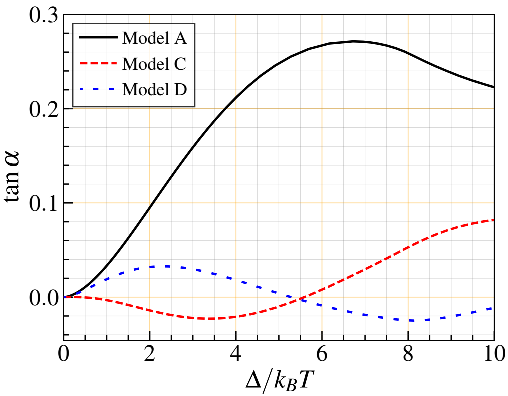

Models E and F: Pöschl-Teller potential

- $U(x) = U_0 / \cosh^2[\alpha x^n], \;\; x = k_f r$

  Model E: $U_0 = 1.01 E_f, \alpha = 3 \times 10^{-5}, n = 4$ Model F: $U_0 = 2 E_f, \alpha = 6 \times 10^{-5}, n = 4$

- $\overleftrightarrow{\mu} = \begin{pmatrix} \mu_\perp & \mu_{\mathrm{AH}} & 0 \\ -\mu_{\mathrm{AH}} & \mu_\perp & 0 \\ 0 & 0 & \mu_\parallel \end{pmatrix}, \;\; \tan\alpha = \frac{\mu_{\mathrm{AH}}}{\mu_\perp}$

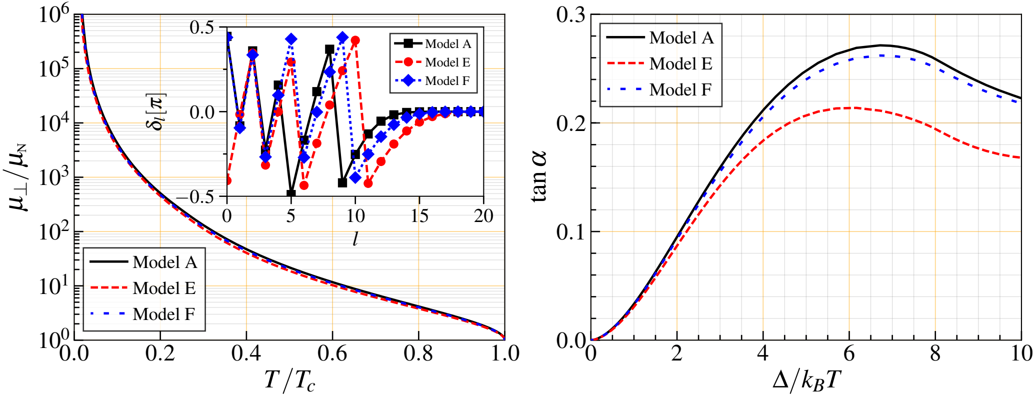

Summary

- Electron bubble is effectively described by a short-range repulsive potential
- Hard-sphere model is in very good agreement with experiments
- Softer, longer range potentials, as well as potentials with intermediate-range attraction, fail to account for the magnitude and temperature dependence of the Hall angle

Thank you!